

STAR FORMATION AND SPIRAL STRUCTURE IN M81

Michele Kaufman¹ and Frank N. Bash²¹Department of Physics
The Ohio State University
Columbus, OH 43210²Department of Astronomy
The University of Texas at Austin
Austin, TX 78712

ABSTRACT. High resolution digitized images of M81 in the radio continuum, H α , H I, and I band are used to see how well various density wave models agree in detail with observations. We find that the observed width of the nonthermal radio arms favors a cloudy version of a density wave model (e.g., the model of Roberts and Hausman). The radial distribution of the set of giant radio H II regions disagrees with the simple expression of Shu and Visser for star formation by a density wave. The observed displacements of the giant radio H II regions from the spiral velocity shock indicate that some revisions in the details of the ballistic particle model of Leisawitz and Bash are necessary.

1. INTRODUCTION

In classical density wave theory, the compression of the gas by a spiral shock is responsible for triggering the formation of new stars. Some recent versions of density wave theories take into account the clumpy nature of the interstellar medium. For example, in the cloudy density wave model of Roberts and Hausman (1984), star formation is enhanced in the spiral arms because collisions between giant clouds occur more frequently there. Digitized high resolution radio and optical images of galaxies can now be made for checking the predictions of these various theories. We selected M81 for such a study because (i) the observed H I velocity contours show a spiral velocity shock (Visser 1980 a,b, Hine and Rots 1986) and thus provide strong evidence for a density wave in this grand design spiral, and (ii) theoretical density-wave models of this galaxy are available from Visser (1980 a,b) and Leisawitz and Bash (1982) for comparison with observations.

We present three tests of density wave models for M81. These tests involve using VLA radio continuum data from Bash and Kaufman (1986), VLA H I data from Hine and Rots (1986), H α observations by Hodge and Kennicutt (1983), and I band data from Elmegreen (1981). We compare these observations of M81 with some predictions of the following density-wave models:

(a) the hydrodynamic density-wave model for M81 by Visser (1980 a,b), who treats the interstellar gas as a continuous, single component medium;

(b) the ballistic particle model for M81 by Leisawitz and Bash (1982), who use Visser's model for the H I gas but assume that stars form in giant clouds that orbit as ballistic particles;

(c) the cloudy density wave model for our Galaxy by Roberts and Hausman (1984), who impose a spiral gravitational perturbation but use an N-body calculation to simulate a cloudy interstellar medium.

The models of Roberts and Hausman and Leisawitz and Bash both involve clouds and a spiral gravitational perturbation but differ in the assumptions made about the clouds and the processes that lead to star formation.

Our goal is to see how well the above models agree in detail with the available data.

2. FIRST TEST: OBSERVED WIDTH OF THE NONTHERMAL RADIO ARMS

Classical density wave theory predicts a narrow nonthermal emission ridge on the inside edge of the spiral arms, where a spiral shock compresses the interstellar gas and magnetic fields. Since M81 is not seen face-on, the width of the ridge in the plane of the sky would depend on the scale height of the shocked layer. If the appropriate shocked layer is the H I disk, then Visser's model predicts a nonthermal ridge that is, at most, 260 pc wide in the plane of the sky. Roberts and Hausman did not do a model for M81. For our Galaxy their model produces a spiral "shock front" 300 - 600 pc wide and a spiral density enhancement 1 kpc wide; we expect that their calculations would yield similar results for M81.

To determine the width of the nonthermal radio arms for comparison with these values, Bash and Kaufman (1986) have made VLA observations of M81 at wavelengths of 6 and 20 cm. We detect radio continuum emission from the spiral arms and the mini-Seyfert nucleus, but not from the disk. On a series of radio continuum and spectral index maps that range in resolution from 10" to 15" (160 - 240 pc if the distance of M81 is 3.3 Mpc), we are able to separate giant H II regions from the more extended nonthermal arm emission (see Figure 1). The good correspondence between H II regions and many of the bright knots on the radio continuum arms is shown in Kaufman et al. (1986), where an H α image is superimposed on a 20 cm radio image, both at a resolution of 10". A spectral index map with a resolution of 18" shows that much of the more extended emission from the arms is mildly nonthermal. Either the extended emission is a combination of nonthermal and diffuse free-free emission or the electron energy spectrum is not very steep. In the latter case, our spectral index values would agree with Duric's (1986) proposed mechanism for diffusive shock acceleration of relativistic electrons by spiral density-wave shocks.

Bash and Kaufman (1986) show examples of intensity profiles obtained by slicing across the radio continuum arms at various positions that avoid the giant H II regions. The intensity profiles were made on a 20 cm map with a resolution of 9.5" (150 pc) and on one with a resolution of 17" (270 pc). On both maps the nonthermal arms are patchy and well resolved, with a typical width of 1 - 2 kpc. Therefore the nonthermal arms are too broad to fit Visser's hydrodynamic model and seem to agree better with the width of the density enhancement in the cloudy density wave model of Roberts and Hausman.

From their VLA H I maps of M81, Hine and Rots (1986) conclude that the observed width of the velocity shock is too broad to agree with Visser's model but appears consistent with the width of the shocked layer in the model of Roberts and Hausman for our Galaxy. Therefore both the synchrotron radiation and the H I data point to the same conclusion.

3. SECOND TEST: THE RADIAL DISTRIBUTION OF GIANT RADIO H II REGIONS IN THE PLANE OF M81

Kaufman et al. (1986) study 42 giant H II regions with high surface brightness that are detected in the radio continuum maps of M81. Figure 1 shows the distribution of these giant radio H II regions deprojected into the plane of M81 and superimposed on a gray-scale display of the deprojected 20 cm map. The set of giant radio H II regions is more sharply confined to the spiral arms than the total optical samples plotted by Connolly et al. (1972) and Hodge and Kennicutt (1983). The total optical sets include faint H II regions as well as bright ones. We conclude that the giant radio H II regions are more likely to be related to a density wave. Rumstay and Kaufman (1983) find a similar phenomenon in M83 and M33 and suggest that the low luminosity H II regions are more likely to occur in smaller clouds and to involve sporadic star formation.

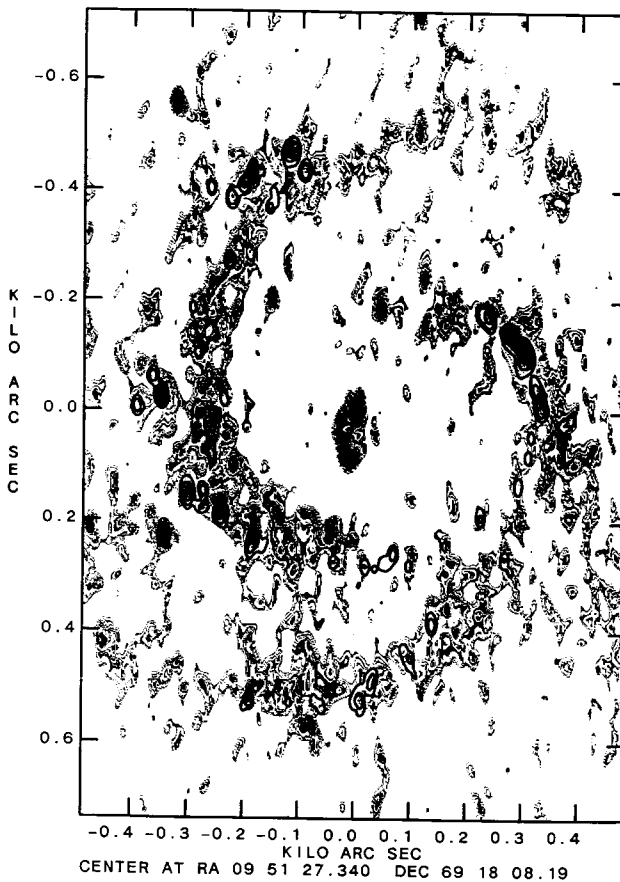


Figure 1. A gray-scale display of the 20 cm emission after deprojection into the plane of M81. The superimposed contours show the positions of the giant H II regions that are detected in the radio. The bright compact source in the nucleus was subtracted before making this map. The major axis is horizontal.

We use the radial distribution of giant radio H II regions in the plane of M81 to test the following simple relation proposed by Shu (1974) for star formation by a density wave:

$$N(\text{H II}) \sim \sigma_{\text{HI}} [\Omega(R) - \Omega_p] (\sigma_{\text{shock}} / \sigma_g)^n, \quad n = 1, 2, \quad (1)$$

where $N(\text{H II})$ is the number of H II regions per kpc^2 , σ_{HI} is the mean surface

density of H I at galactocentric distance R , $\Omega(R)$ is the angular rotation speed of the matter, Ω_p is the pattern speed, and $\sigma_{\text{shock}}/\sigma_g$ is the spiral shock compression of the gas. The lower bar graph in Figure 2 is the observed radial distribution of the set of giant radio H II regions, while the dashed curve is obtained from Shu's expression with parameter values from the Visser model that gives the best fit to the observed distribution. Although the peak occurs at about the same location in both distributions, the observed distribution is more sharply peaked than the predicted one.

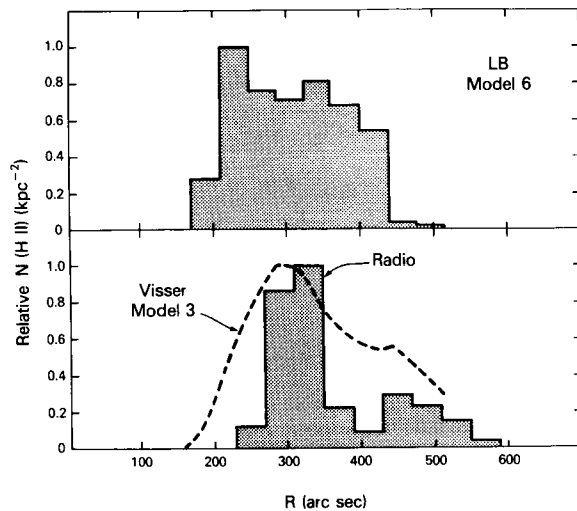


Figure 2. Comparison of the observed radial distribution of the set of giant radio H II regions (the bar graph labeled "radio") with the predictions of models for M81 by Visser (1980b) and Leisawitz and Bash (1982).

CO measurements and upper limits suggest that the surface density of H_2 in M81 is very low; therefore replacing σ_{HI} in Equation (1) by the surface density of atomic plus molecular hydrogen would not change the clear disagreement between theory and observation. We know of only one convincing detection of CO in M81: using a 102" FWHP beam (1.6 kpc at the distance of M81) centered near the two most luminous H II regions in the peak of the radial distribution, Stark (1986) obtains an integrated Δv of only 0.3 ± 0.1 $K km s^{-1}$ for the $J = 1 \rightarrow 0$ transition of ^{12}CO . This suggests that H_2 is a very minor constituent compared to H I.

The upper bar graph in Figure 2 is the prediction of a ballistic particle model adopted by Leisawitz and Bash for M81; it disagrees with our observations. To get their model to produce the narrow peak in the observed radial distribution requires a different choice for the assumed radial distributions of either the small clouds or of the birth sites of the giant clouds.

4. THIRD TEST: THE LOCATIONS OF THE SPIRAL ARMS DEFINED BY VARIOUS TRACERS

Figure 3 shows the H I intensity data from Hine and Rots (1986) after deprojection into the plane of M81, with the major axis horizontal. Rots (1975) suggests that the faint inner H I ring is produced by the inner Lindblad resonance. Our 20 cm observations support this interpretation (see Bash and Kaufman 1986). The position of the velocity shock measured by Hine and Rots is along the inside edge of the H I arms. Notice that the inner edge

of the arms is more sharply defined than the outer (downstream) edge. Near the northern major axis (the left-hand side in Fig. 3), the H I arm spreads out. This may be the result of a tidal distortion by M82.

Elmegreen's (1981) I band plate shows the spiral arms defined by the old stars; the I band ridge indicates the location of the spiral potential minimum. When we superimpose a sharp-masked I band image on the H I image, we see that the potential minimum defined by the old stars lies just downstream from the spiral shock. This agrees qualitatively with Visser's hydrodynamic model and with the cloudy density wave model of Roberts and Hausman. Figure 3 shows the positions of the giant H II regions that are detected in the radio. All but one of the giant radio H II regions are located on either the H I arms or the inner H I ring. Essentially all of these regions lie downstream from

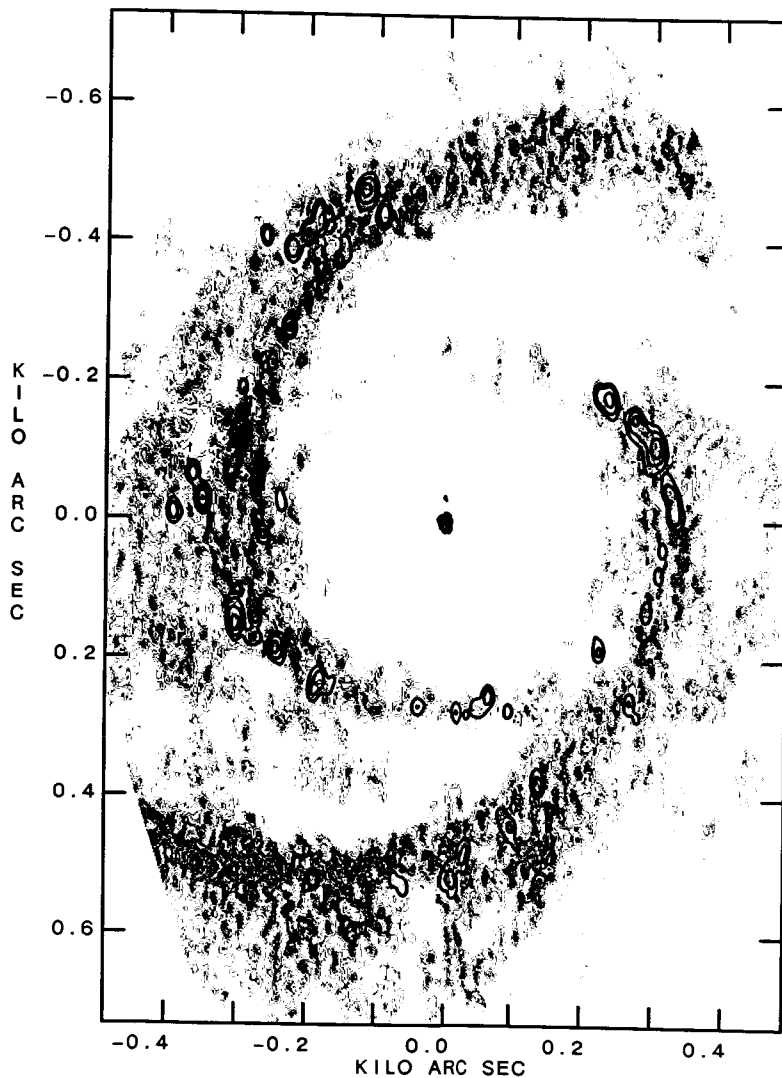


Figure 3. A gray-scale display of the rectified H I intensity map from Hine and Rots (1986). The superimposed contours show the locations of the giant radio H II regions. The compact nucleus is not an OB association but is retained here as a fiducial point. The major axis is horizontal.

the spiral shock. If the H I image, the distribution of giant radio H II regions, and the sharp-masked I band image are all superimposed (as was shown in a colored slide in the lecture), then one sees that some of the giant radio H II regions lie along the potential minimum defined by the old stars; the others, particularly at large R, are farther downstream.

To illustrate how this data can be used to test density wave models, we consider the angular distribution of H II regions that Leisawitz and Bash obtain with their adopted ballistic particle model for M81. Near the major axis, the model predicts two clumps of H II regions: one just upstream from the shock and the other stretching appreciably downstream. Near the southern major axis all the observed giant H II regions lie along the spiral potential minimum (i.e., just downstream from the shock); near the northern major axis some are located still farther downstream. At large galactocentric R, the model predicts that all H II regions should lie just upstream from the shock, but here the observed regions are significantly downstream from the shock. It appears that some change is required in the values used in their model for the launch speed and the time delay before the onset of star formation.

5. CONCLUSIONS

The observations of M81 are consistent with the presence of a density wave; this paper is concerned with how well the details fit. The width of the nonthermal radio arms favors a cloudy version of a density wave model. A comparison between the predictions of the ballistic particle model of Leisawitz and Bash (1982) and the observed radial and azimuthal distributions of giant radio H II regions indicates that some revision in the details of their model is necessary.

ACKNOWLEDGMENTS. We thank Butler Hine, Arnold Rots, Debra Elmegreen, Robert Kennicutt, and Paul Hodge for supplying us with copies of their digitized data. We thank Burton Jones for measuring the α , δ coordinates of the bootstrap standard stars that we used in doing the plate solutions. We thank Tony Stark for providing his unpublished results. This paper was written while M.K. held a National Research Council - NASA Research Associateship at Goddard Space Flight Center, Greenbelt, MD.

The National Radio Astronomy Observatory is operated by Associated Universities, Inc., under contract with the National Science Foundation. We thank the NRAO staff for this assistance.

REFERENCES

- Bash, F.N., and Kaufman, M. 1986, Ap.J., in press.
 Connolly, L.P., Mantarakis, P.Z., and Thompson, L.A. 1972, Pub. A. S. P., 84, 61.
 Duric, N. 1986, Ap.J., 304, 96.
 Elmegreen, D.M. 1981, Ap. J. Suppl., 47, 229.
 Hine, B., and Rots, A.H. 1986, in preparation.
 Hodge, P.W., and Kennicutt, R.C. 1983, Ap. J., 267, 563.

- Kaufman, M., Bash, F.N., Kennicutt, R.C., and Hodge, P.W. 1986, preprint.
 Leisawitz, D., and Bash, F.N. 1982, Ap. J., 259, 133.
 Roberts, W.W., and Hausman, M.A. 1984, Ap. J., 277, 744.
 Rots, A.H. 1975, Astr. Ap., 45, 43.
 Rumstay, K.S., and Kaufman, M. 1983, Ap. J., 274, 611.
 Shu, F.H. 1974, in The Interstellar Medium, ed. K. Pinkau (Dordrecht: Reidel),
 p. 219.
 Stark, A.A. 1986, private communication.
 Visser, H.C.D. 1980a, Astr. Ap., 88, 149.
 _____. 1980b, Astr. Ap., 88, 159.

DISCUSSION

DICKEY:

I was not surprised to see a mixture of thermal and non-thermal emission shown by the spectral index map for the south-eastern spiral arm, but I was surprised that there is not a gradient in the spectral index representing a variation in the mixture of thermal and non-thermal emission. Are you confident that you have resolved the spiral arm?

KAUFMAN:

First of all, this is VLA data, not data taken with a filled aperture, so one should exercise some caution in interpreting the spectral index values. We checked on a spectral index map made with 160 pc resolution that the bright H α sources have spectral indices consistent with optically-thin free-free emission. The slide showed a spectral index map with a resolution of 290 pc, and at this lower resolution the emission from an HII region is convolved with surrounding non-thermal arm emission. We use this map to distinguish between free-free, mildly non-thermal, and strongly non-thermal emission, but I would be wary of making finer distinctions. We find that most of the extended arm emission is mildly non-thermal.

Secondly, the intensity profiles across the arms show that the arm emission is resolved.